Blended Calcium Sulfoaluminate Cements Based on Thermally Treated Reservoir Sediments

Antonio Telesca * and Milena Marroccoli *

Posted Date: 11 January 2024

doi: 10.20944/preprints202401.0879.v1

Keywords: calcium sulfoaluminate cements; thermally treated reservoir sediments; supplementary cementitious materials; hydration; expansion; mechanical strength

Article

Blended Calcium Sulfoaluminate Cements Based on Thermally Treated Reservoir Sediments

Antonio Telesca [1] and Milena Marroccoli [2,*]

[1] School of Engineering, University of Basilicata, Via Ateneo Lucano 10, 85100 Potenza, Italy; antonio.telesca@unibas.it 1
[2] School of Engineering, University of Basilicata, Via Ateneo Lucano 10, 85100 Potenza, Italy
* Correspondence: milena.marroccoli@unibas.it

Abstract: In 2021 about 4.1 billion tonnes of cement were produced overall in the world and the annual CO_2 emissions from cement plants reached almost 2.8 billion metric tonnes. In the last years many efforts have been made for manufacturing low-CO_2 cements. In this regard, a great consideration has been addressed towards calcium sulfoaluminate (CSA) binders for both their peculiar technical features and the sustainable properties principally connected to their industrial process. Moreover, the use of blended cements composed by CSA binders and supplementary cementitious materials can be an effective way to a) reduce the CO_2 footprint and b) to produce greener cement binders. This scientific work studied the utilization of calcined reservoir sediments (RS) as supplementary cementitious materials in blended-CSA binders. Four cements were subjected to hydration and physical investigations for curing times included in the interval 4 hours-56 days. X-ray fluorescence, X-ray diffraction and thermogravimetric analyses were employed as main characterization techniques. It was found that thermally treated RS are particularly noteworthy as their utilization allows a dilution of CSA clinker, thus implying a decrease of CO_2 emissions and a reduction of costs related to CSA cement production.

Keywords: calcium sulfoaluminate cements; thermally treated reservoir sediments; supplementary cementitious materials; hydration; expansion; mechanical strength

1. Introduction

The cement manufacturing process is one of the main contributors to global warming as well as climate change [1]. In 2021 approximately 4.1 billion tonnes of cement were manufactured [2] and the total carbon dioxide produced in cement plants was equal to approximately 2.8 billion metric tonnes, namely about 7% of global anthropogenic CO_2 emissions [3]. Nowadays the cement industry is aimed at lowering the CO_2 emissions to 1.55 billion metric tonnes/year by the end of 2050 [4]; therefore, cement producers and the researchers are looking for new hydraulic binders manufactured with reduced CO_2 emissions (low-CO_2 cements) [5-14]. Low-CO_2 cements can be manufactured using three different modes, that is: I) the utilization of non-carbonated sources of calcium oxide for limestone in the raw mix for the synthesis of Portland clinker [15-16]; II) the increased production of ordinary Portland cement (OPC) blended with supplementary cementitious materials (SCMs) [17-18]; and III) a wider employment of special binders (SCs), namely cements produced from non-Portland clinkers [19-20].

SCs display peculiar technical properties useful in specific fields of application; in addition, their composition can be exploited to give more environmentally friendly features to their production process. Nowadays, there is a noticeable interest towards calcium sulfoaluminate (CSA) cements for their relevant technical properties [21-32] coupled with environmentally friendly features [33-35]. CSA cements are obtained by mixing a clinker (derived from heating a meal composed by natural gypsum, bauxite and limestone) with a source of calcium sulfate (e.g. anhydrite, natural gypsum); CSA binders contain calcium sulfoaluminate ($3CaO{\cdot}3Al_2O_3{\cdot}CaSO_4$, ye'elimite) as principal constituent and, on the basis of the burning temperature, type and proportion of raw materials, calcium sulfates, dicalcium silicate ($2CaO{\cdot}SiO_2$, belite), calcium aluminium ferrite (brownmillerite,

 doi:10.20944/preprints202401.0879.v1

$4CaO{\cdot}Al_2O_3{\cdot}Fe_2O_3$) calcium sulfosilicate (sulfospurrite, $4CaO{\cdot}2SiO_2{\cdot}CaSO_4$) and several calcium aluminates.

The CSA cements technical features (e.g. rapid hardening, high impermeability, excellent dimensional stability) are mainly due to the ye'elimite hydration with $CaSO_4$c which lead the formation of $3CaO{\cdot}Al_2O_3{\cdot}3CaSO_4{\cdot}32H_2O$ (ettringite) [20].

Compared to ordinary Portland cement, CSA cements display the following sustainable characteristics: 1) reduced synthesis temperatures (<1350°C); 2) lower limestone requirement (usually <35%) in the clinker-generating raw meal; 3) lower energy for the cement milling; and 4) wider utilization of industrial wastes in the cement manufacturing process [36-44]. In order to further decrease the generation of CO_2 and reduce their high costs (mainly depending on the utilization of bauxite), CSA cements can be blended with SCMs [45-53].

Water reservoirs store fresh water which is generally piped to electric power stations and/or used for drinking as well as irrigation. The most important issues for these basins are silting phenomena which cause the reduction of the original storage capacity. To recover the original capacity, dredging operations are carried out: they generate large amounts of sediments which are generally landfilled. The research conducted so far to avoid the landfill, has evaluated the utilization of dredged sediments for the manufacture production of lightweight aggregates, Portland cement clinker, bricks, as component for stabilized road-base as well as supplementary cementitious material in blended cements [54-56].

This paper aimed at investigating the use of thermally treated (TT) clayish reservoir sediments (RS) as SCM in blended CSA binders; the best treatment temperature (BT) allows the total conversion of crystalline clay phases in amorphous constituents (process of dehydroxylation) [57]. Four $TTRS_{BT}$-based CSA binders were investigated by means of hydration and physical-mechanical tests for curing times falling within the interval 4 hours - 56 days. A plain CSA binder was employed as a benchmark. The effect of $TTRS_{BT}$ on both hydration evolution and technical behaviour of CSA-blended binders was evaluated by using differential-thermal-thermogravimetric (DT-TG) and X-ray diffraction (XRD) measurements coupled with mercury intrusion porosimetry (MIP), dimensional stability and mechanical tests.

2. Materials and Methods

2.1. Materials

An Italian cement manufacturer supplied the calcium sulfoaluminate binder; RS came from the "Camastra" basin in Basilicata (Italy). Six sediments samples were taken from different locations within the bottom of the reservoir; they were heated at 110°C to remove the surface moisture; afterwards, they were mixed all together an milled to pass A 90 μm sieve.

2.2. Methods and Evaluation Techniques

Three 100 g batches of RS were heated in a fix electric oven for 120 minutes at 750°, 830° and 900°±2°C for evaluating the BT which allows the total dehydroxylation; the resulting materials were finely ground below 90 μm in the FP6 mill (10 minutes at 450 rotations per minute) and characterized by XRD analysis.

The chemical analyses of CSA binder, RS and TTRS (obtained at the optimal synthesis temperature, $TTRS_{BT}$), determined through the X-ray fluorescence equipment (Explorer S4- BRUKER), are displayed in Table 1 together with the most important CSA cement mineralogical phases are also shown. The XRD patterns of RS and the three TTRS (FIG. 1) were collected using a MINFLEX 600 (RIGAKU) diffractometer with CuKα radiation and scan rate of 0.02°/step.

Four CSA-based cements were examined: a pure CSA cement (C_R) and three CSA binders containing $TTRS_{BT}$ as substitute for part of C_R (15%, 25% and 35% by mass, C_15, C_25 and C_35, respectively). Cementitious pastes were obtained employing a water to cement (w/c) ratio of 0.50; they were transferred into plastic cylindrical containers and stored in a thermostatically-controlled water (20°C). After each chosen curing period (comprised in the interval 4 hours to 56 days), the hardened cylindric pastes were broken in 2–parts: one piece underwent MIP analysis (Thermo-Finnigan Pascal 240 and 140 Series porosimeters), the other one was milled (grain size <90μm) for

 doi:10.20944/preprints202401.0879.v1

DT-TG (using a NETZCH-TASC 414/3 equipment operating at 10°C/min in air) and XRD (using a Bruker D4 Endeavor apparatus wiht CuKα-radiation and scan rate of 0.02/step) analyses. The hydration stoppage was carried out by means of a solvent exchange method employing acetone (to remove free water) and diethyl ether (to reduce the acetone evaporation time); finally, hardened samples were stored in a desiccator over silica gel and soda lime to mitigate the action of water vapour and carbonation, respectively.

For the dimensional stability (expansion–shrinkage) tests, 24 prisms of cementitious paste (15X15X78 mm) were put in air at ambient temperature for 24 hours and afterwards demoulded. For each system, three prisms were submerged in water at 20°C, and the other three left in a thermostatically controlled equipment (20°C, 65% relative humidity). A mechanical length comparator device was employed to determine the dimension of the paste samples at various hydration time. The mean length value was then calculated as the average of the three measurements.

Cement mortars, realized in accordance with the European Standard EN 196-1, were subjected to compressive strength tests at curing times falling in the range 4 hours-56 days.

3. Results

The chemical analysis for CSA cement, RS and $TTRS_{BT}$ is illustrated in Table 1 which also shows the mineralogical composition of the binder evaluated by the Rietveld method (normalizing the results to only the detected crystalline phases).

Table 1. Chemical and phase compositions (solely for C_R) of the employed cement components, mass %.

Chemical composition				Mineralogical phase composition		
	CSA cement	RS	$TTRS_{BT}$	CSA cement	ICDD ref. number	
CaO	44.58	9.05	10.10	Ye'elimite	30-0256	43.0
SiO_2	8.95	51.86	58.11	β-belite	33-0302	21.7
Al_2O_3	22.42	13.48	15.26	Celite	38-1429	3.8
Fe_2O_3	1.86	5.16	5.10	Anhydrite	37-1496	19.1
TiO_2	1.10	0.65	0.76	Calcite	05-0586	1.1
K_2O	0.30	1.74	1.94	Brownmillerite	30-0256	4.5
MnO	0.08	0.15	0.17	Gehlenite	73-2041	1.6
Na_2O	0.08	0.81	0.90	Others		5.2
MgO	0.94	2.04	2.26			
SO_3	16.85	0.22	0.46			
P_2O_5	0.05	0.15	0.18			
l.o.i*	2.16	14.5	2.70			
Total	99.37	99.78	97.94	Total		100.0

* l.o.i=loss on ignition evaluated at 950°±10°C

The chemical analysis on C_R reveals calcium, aluminium, sulfur and silicon oxides are, in the order its main components. Moreover, the Rietveld evaluation denotes that $4CaO{\cdot}3Al_2O_3{\cdot}SO_3$ (43.0 mass%), β-$2CaO{\cdot}SiO_2$, $4CaO{\cdot}Al_2O_3{\cdot}Fe_2O_3$, $3CaO{\cdot}Al_2O_3$ (tricalcium aluminate) and $2CaO{\cdot}Al_2O_3{\cdot}SiO_2$ (gehlenite), are, in the order, its main crystalline components; $CaSO_4$, mainly coming from the added natural anhydrite to the clinker, is also present. As far as the reservoir sediments are concerned, from the results of the chemical composition, it is found that silicon and aluminum oxides represent their principal components; additionally, CaO, as also revealed by DT-TG investigation, is present as $CaCO_3$. Therefore, the RS l.o.i. is due to both CO_2 and water of the argillaceous minerals.

Figure 1 displays the XRD patterns for RS together with its corresponding thermally treated (at 750°, 830° and 900°C) materials.

Preprints (www.preprints.org) | NOT PEER-REVIEWED | Posted: 11 January 2024 doi:10.20944/preprints202401.0879.v1

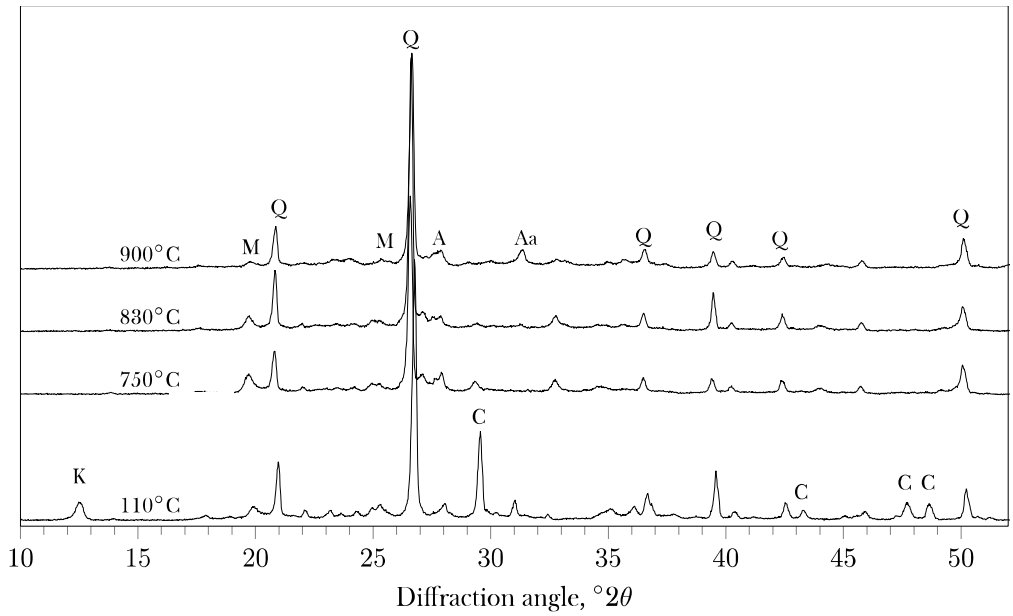

Figure 1. XRD patterns for RS and the corresponding samples burnt from 750° to 900°C. Aa=alumoakermanite ($(Ca,Na)_2(Al,Mg,Fe^{++})(Si_2O_7)$); A=anorthite ($CaAl_2Si_2O_8$); C=calcite ($CaCO_3$); K=kaolinite ($Al_2Si_2O_5(OH)_4$); M=muscovite ($KAl_2(Si_3Al)O_{10}(OH,F)_2$); Q=quartz ($SiO_2$).

Muscovite, kaolinite, quartz and calcite are the key-crystalline components for RS; XRD patterns for the TTRS display: I) the disappearance of kaolinite already at 750°C; II) the reduction of muscovite with temperature; and III) the presence of alumoakermanite (identified for the first time at 830°C) whose main peak increases as temperature rises. Consequently, 830°C (BT) represents the best temperature for avoiding the generation of novel unwanted phases coupled with the disappearance of phases already present.

The Blaine specific surface areas (EN 196-6) are 4500 for CSA and 3750 cm^2/g $TTRS_{BT}$.

Figure 2 reports the DT results for C_R, C_15, C_25 and C_35 cured at 4 hours and 1, 28 and 56 days. From the data published on [58], the following endothermal effects (in the order of increasing temperature) were assigned to ettringite (E) and $Al(OH)_3$ (aluminium hydroxide, AH).

Except for the peak of $CaCO_3$, no relevant thermal (exo/endo) effects are present over 500°C; for the examined cement pastes the endothermal dehydration peaks, attributed to E and AH (already detectable after 4 hours of hydration), are respectively observed at 164°±5°C and 287°±4°C.

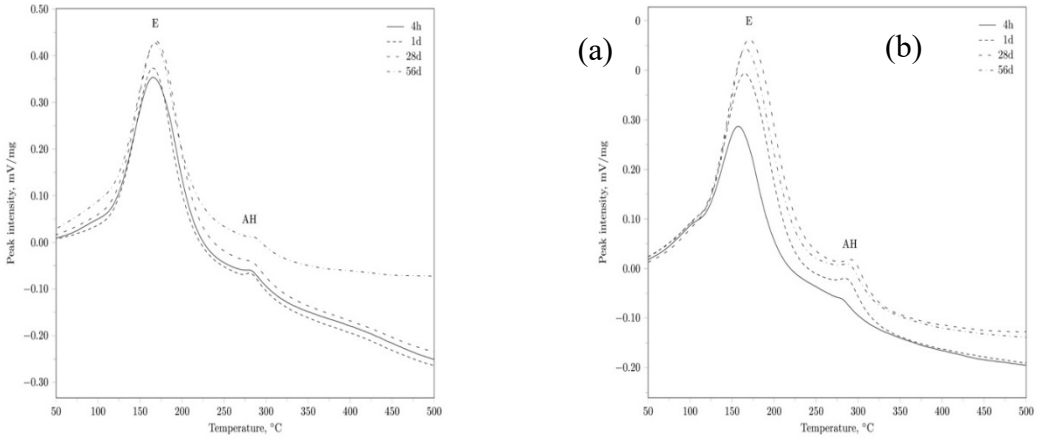

Preprints (www.preprints.org) | NOT PEER-REVIEWED | Posted: 11 January 2024 doi:10.20944/preprints202401.0879.v1

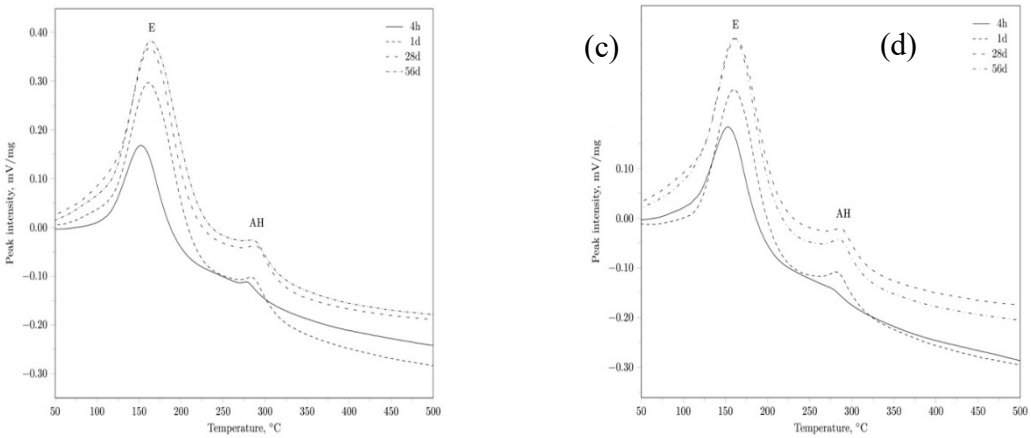

Figure 2. DT curves for cement pastes (a) C_R, (b) C_15 (b), (c) C_25 and (d) C_35 at 4 hours, 1, 28, and 56 days of hydration. E=ettringite; AH=aluminium hydroxide.

Overall, the thermogravimetric analyses reveal that the hydration behaviour is basically due to the reaction of $4CaO{\cdot}3Al_2O_3{\cdot}SO_3$ with $CaSO_4$. The hydration behaviour of the systems was also assessed by means of the determination of the bound water content (CBW, Figure 3); it was evaluated considering the weight loss values to 500°C and normalized to 100 g dry cement.

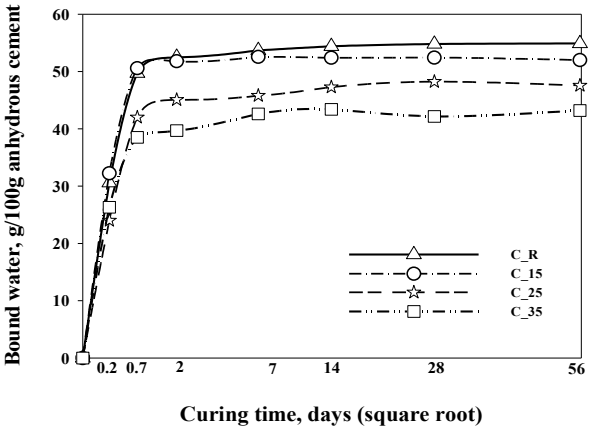

Figure 3. Chemical bound water calculated by TG until 56 days of aging (g/100 g of unhydrous cement) for C_R, C_15, C_25 and C_35 cements pastes *vs* aging time.

From Figure 3 it can be argued that the 4 systems follow an analogous trend during the first 24 h; at that period the hydration rate is quite high because of the fast ettringite formation; from 7 days of curing, the curves exhibit an almost constant value.

XRD patterns (Figure 4) almost confirm the indications obtained from both DT analyses and bound water results; therefore, concerning the hydration products, ye'elimite and calcium sulfate fast react and $3CaO{\cdot}Al_2O_3{\cdot}3CaSO_4{\cdot}32H_2O$ concentration grew up to 28 days of aging; the aluminium hydroxide main peak is also found in all the hydrated systems.

Preprints (www.preprints.org) | NOT PEER-REVIEWED | Posted: 11 January 2024 doi:10.20944/preprints202401.0879.v1

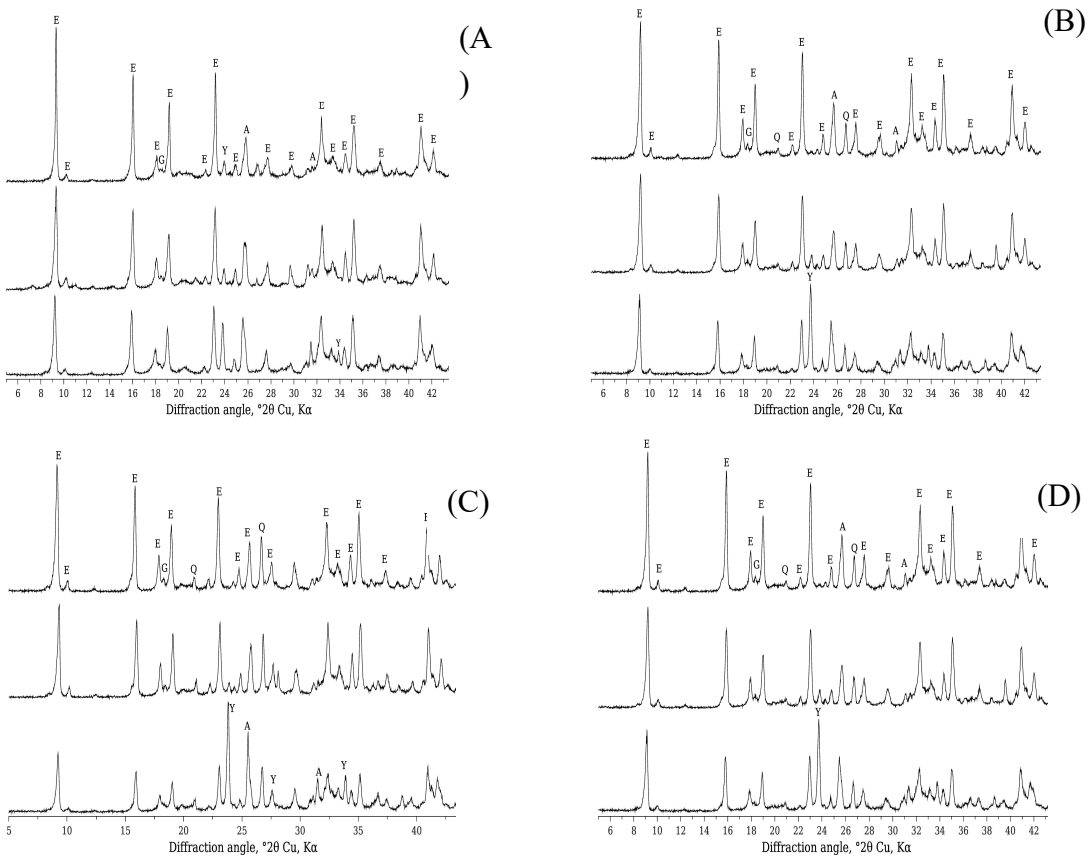

Figure 4. XRD patterns of C_R (A), C_15 (B), C_25 (C) and C_35 (D) hydrated for 4 (down) hours and 2 (middle) and 28 (up) days. A=anhydrite; E=ettringite; G=aluminium hydroxide; Q=quartz; Y=ye'elimite.

Furthermore, belite was virtually not involved in the hydration process, owing to both the higher reaction kinetics of calcium sulfoaluminate and the related rapid water consumption. Quartz signals, already present in the TTRSBT samples, are detected in all the investigated CSA-blended cements. Figure 5 shows the evolution of ettringite *vs.* curing time. Elevated quantities of ettringite already forms after 4 hours of hydration in all the systems; after 2 days, the $3CaO{\cdot}Al_2O_3{\cdot}3CaSO_4{\cdot}32H_2O$ concentration reaches almost its maximum value and, since then, sliglthly rises until 28 days of curing.

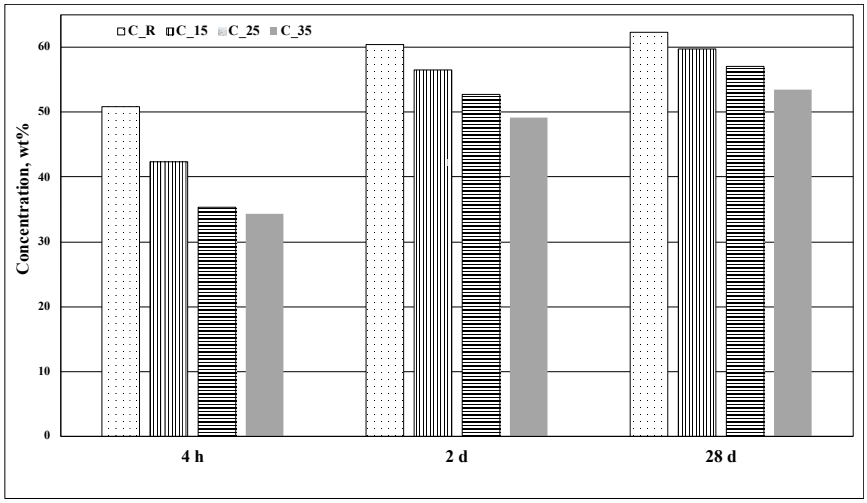

Figure 5. Ettringite concentration (evaluated by means of the Rietveld analysis) for C_R, C_15, C_25 and C_35 evaluated in the interval 4 hours-28 days.

Preprints (www.preprints.org) | NOT PEER-REVIEWED | Posted: 11 January 2024 doi:10.20944/preprints202401.0879.v1

The curves related to the expansion (under water)–shrinkage (in air) tests are reported in Figure 6.

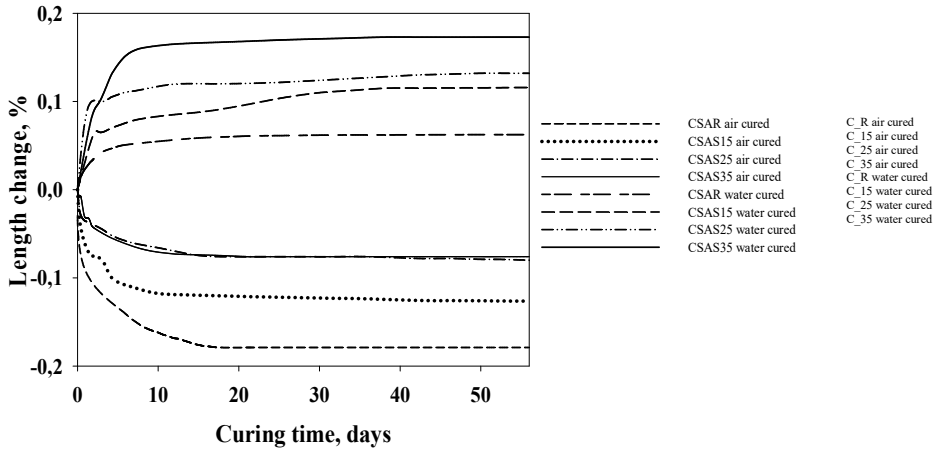

Figure 6. Expansion/shrinkage plots for the four CSA systems (cured in water and in air).

Both in air and submerged under water, the behaviour of the three blended cements was almost similar to each other and to that of the reference system. When aged in air it is evident a constant shrinkage until nearly 2 weeks, when a lowest value is attained (-0.18%, -0.13%, -0.08% and -0.07% for C_R, C_15, C_25 and C_35, respectively); afterwards, the shrinkage results are almost consistent. The highest values of expansion under water, reached after approximately 20 days of aging, are included in the range 0.06-0.17%.

In Figure 7 the plots of the porosimetric tests for the pastes of the four examined cements are reported; its left and the right side respectively represent the derivative and cumulative pore volume (CPV) curves related to the intruded mercury for calcium sulfoaluminate-based cements towards pore radius for aging periods ranging comprised in the interval 16 hours-56 days. For C_R (Figure 7 (A)), all the derivative plots display a unimodal distribution [20].

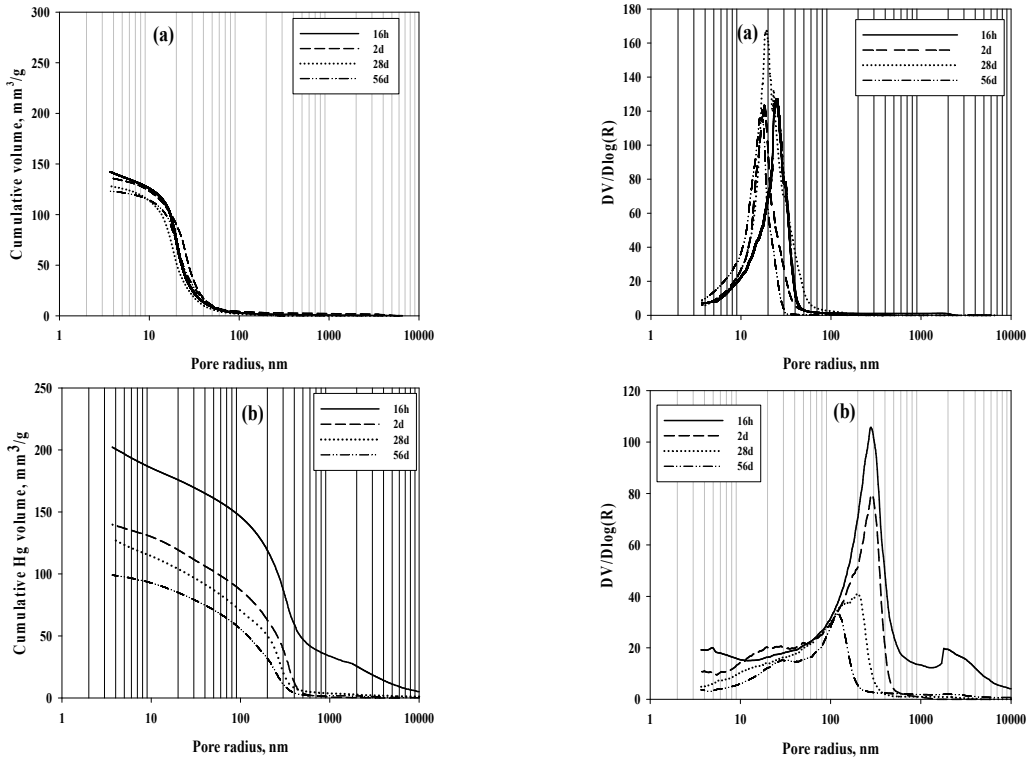

Preprints (www.preprints.org) | NOT PEER-REVIEWED | Posted: 11 January 2024 doi:10.20944/preprints202401.0879.v1

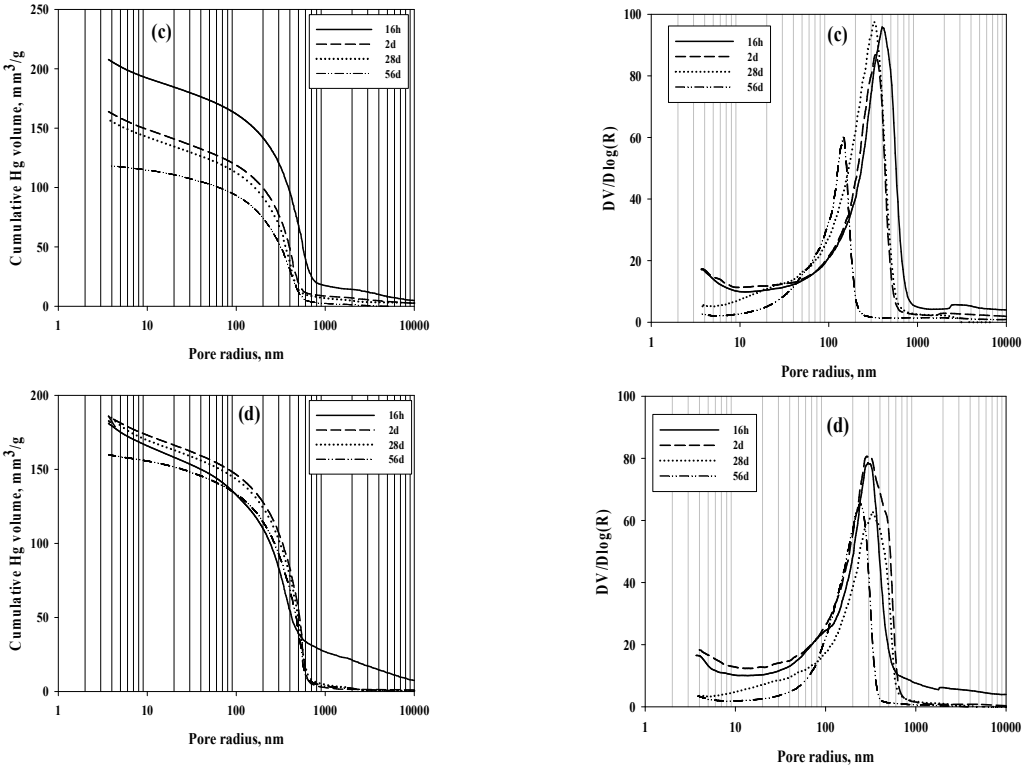

Figure 7. Derivative (right) and cumulative (left) mercury intruded volume *vs.* pore radius for C_R (a), C_15 (b), C_25 (c) and C_35 (d) hydrated for 16 hours and 2, 28, 56 days.

Over the aging period, the CPV as well as the threshold pore radius slightly reduce (from 142 to 123 mm^3/g and from nearly 25 to 16 nm, respectively). Compared to C_R, the $TTRS_{BT}$-based cements show a similar behaviour; in fact, a unimodal pore size distribution is observed at any examined aging period. Moreover, for C_15, the CPV decreases of nearly 30% passing from 201 (at 16 hours) to 140 mm^3/g (after 2 days); at longer aging times it further reduces (about 100 mm^3/g after 56 days of hydration). Similarly, the pore width ranges from 274 (at 16 hours) to 120 nm (at 56 days). For C_25 and C_35, the CPV respectively lowers of approximately 39% and 16% (going from 207 to 118 mm^3/g and from 190 to 160 mm^3/g, respectively) in the same time interval; compared to C_15, C_25 and C_35 exhibit a pore size distribution oriented towards higher radii at all the investigated curing times, being respectively comprised in the intervals 315-160 nm and 400-240 nm.

As a consequence of the fast hydration products generation in C_R (revealed by both XRD and DT-TG analyses), a region of lower porosity is quickly stated; therefore, the hydration products lower and separate the inner space. At higher aging periods, the porosity development goes gradually inasmuch as the hydration has approximately stopped. Due to the lack of phases (e.g. calcium hydroxide) able to react with thermally treated reservoir sediments the investigated blended cements, in comparison with C_R, always display a higher pore size distributions.

The total porosity percentage (TP) results *vs.* of aging period related to the four investigated cements are displayed in Figure 8; the histograms evidently display a comparable trend for all cement pastes inasmuch as their TP values lower as curing time increases.

Preprints (www.preprints.org) | NOT PEER-REVIEWED | Posted: 11 January 2024 doi:10.20944/preprints202401.0879.v1

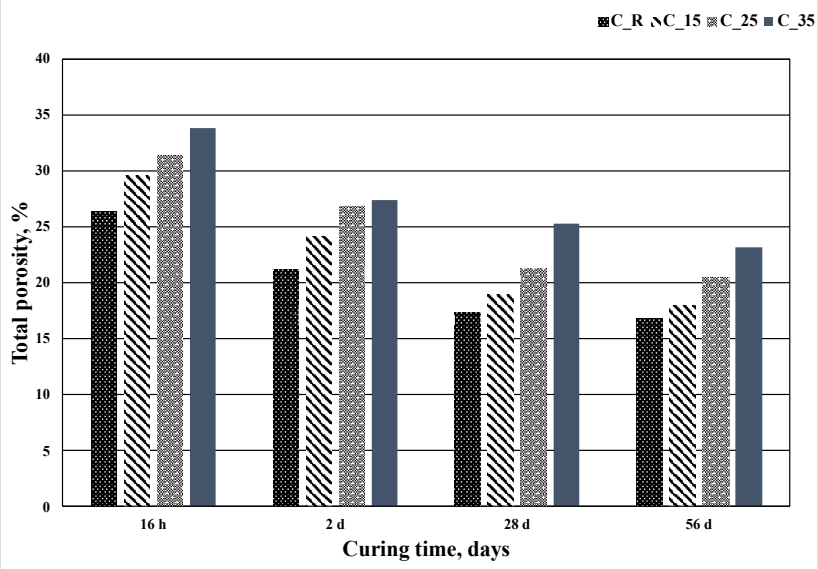

Figure 8. TP for C_R, C_15, C_25 and C_35 pastes hydrated for 16 hours, 2, 28 and 56 days.

In particular, at all the hydrations periods the plain CSA shows the lowest TP values; moreover, it is evident that the higher CSA cement substitution the higher TP values. At the last investigated period, the total porosity for C_35 (23.2%) was about 13% and 30% higher than those exhibited by C_25 and C_15, respectively.

In Figure 9 the compressive strength results for calcium sulfoaluminate-based mortars are reported; the strength results for the 3 blended binders were always lower than those for C_R.

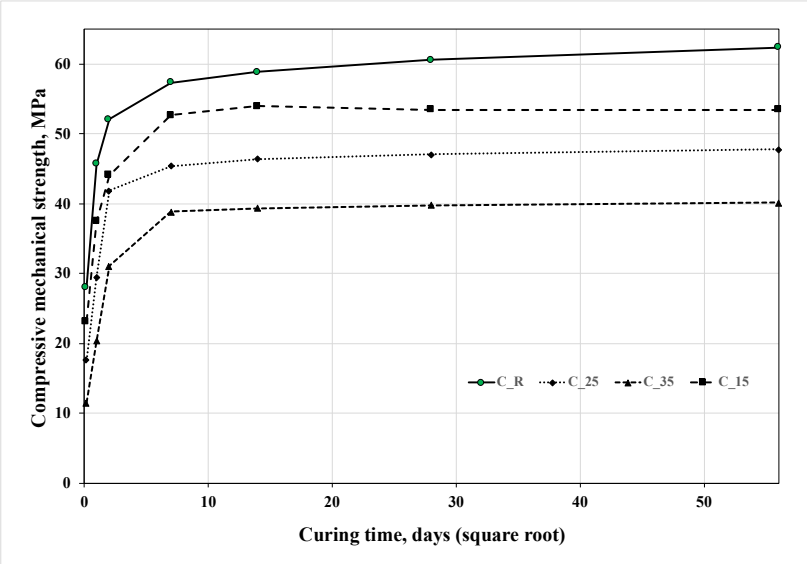

Figure 9. Results of compressive mechanical tests of C_R, C_15, C_25 and C_35 at different curing times.

As the amount of TTRS in the blends increases, the compressive strength values decreases, thus revealing an almost inert behaviour of the reservoir sediments: this phenomenon is most probably due to the lack of a lime source able to react with the TTRS$_{BT}$ amorphous silica and alumina in the cement pastes.

4. Concluding remarks

The work assesses the feasibility of utilizing clayish reservoir sediments (RS) as SCM (supplementary cementitious material) in CSA (calcium-sulfoaluminate) cements. RS were heated

(TT) at 830° for obtaining amorphous constituents thank to the dehydroxylation the silico-aluminate crystalline components.

When compared to plain CSA cement pastes and mortars, those based on blended CSA binders show an increased pore size distribution (as evidenced by mercury intrusion investigations) and a strength reduction with the increase of TTRS replacement levels. In addition, X-ray diffraction and differential thermal-thermogravimetric results show that the presence of thermally treated clayish reservoir sediments affect neither the creation of CSA hydration products nor the dimensional stability of cement pastes (both when cured in water and in air).

The utilization of TTRS as SCM allows both the reduction of the use of natural materials and prevent the landfilling of wastes; in addition, it permits the dilution of CSA cement which implicates both reduced emissions of CO_2 as well as evident energy cut per unit mass of binder.

Author Contributions: A.T.: conceptualization; methodology; formal analysis; investigation; data curation; writing—original draft preparation; writing—review and editing. M.M.: conceptualization; methodology; formal analysis; investigation; data curation; writing—original draft preparation; writing—review and editing. All authors have read and agreed to the published version of the manuscript.

Funding: This research received no external funding.

Institutional Review Board Statement: Not applicable.

Informed Consent Statement: Not applicable. Written informed consent for publication must be obtained from participating patients who can be identified (including by the patients themselves). Please state "Written informed consent has been obtained from the patient(s) to publish this paper" if applicable.

Data Availability Statement: Not applicable.

Conflicts of Interest: The authors declare no conflict of interest.

References

1. Telesca, A.; Ibris, N.; Marroccoli, M. Use of Potabilized Water Sludge in the Production of Low-Energy Blended Calcium Sulfoaluminate Cements. Appl. Sci. **2021**, 11, 1679, doi.org/10.3390/app11041679.
2. Cembureau. **2022**. Activity report 2022. Cembureau, The European Cement Association.
3. IEA. **2023**. Available online: https://www.iea.org/data-and-statistics/charts/direct-emissions-intensity-of-cement-production-in-the-net-zero-scenario-2015-2030, 2022 (Last accessed on 24th November 2023).
4. Barcelo, L.; Kline, J.; Walenta, G.; Gartner, E. Cement and carbon emissions. Mater. Struct. **2014**, 47, 1055–1065, doi:10.1617/s11527-013-0114-5.
5. Schneider, M. The cement industry on the way to a low-carbon future. Cem. Concr. Res. **2019**, 124, 105792, doi:10.1016/j.cemconres.2019.105792.
6. Shi, C.; Qu, B.; Provis, J.L. Recent progress in low-carbon binders. Cem. Concr. Res. **2019**, 122, 227–250, doi:10.1016/j.cemconres.2019.05.009.
7. Gartner, E.; Sui, T. Alternative cement clinkers. Cem. Concr. Res. **2018**, 114, 27–39, doi:10.1016/j.cemconres.2017.02.002.
8. Tregambi, C.; Solimene, R.; Montagnaro, F.; Salatino, P.; Marroccoli, M.; Ibris, N.; Telesca, A. Solar-driven production of lime for ordinary Portland cement formulation. Sol. Energy **2018**, 173, 759–768, doi:10.1016/j.solener.2018.08.018.
9. Gartner, E.; Hirao, H. A review of alternative approaches to the reduction of CO_2 emissions associated with the manufacture of the binder phase in concrete. Cem. Concr. Res. **2015**, 78, 126–142, doi:10.1016/j.cemconres.2015.04.012.
10. Juenger, M.C.G.; Winnefeld, F.; Provis, J.L.; Ideker, J.H. Advances in alternative cementitious binders. Cem. Concr. Res. **2011**, 41, 1232–1243, doi:10.1016/j.cemconres.2010.11.012.
11. Dung, N.T.; Unluer, C. Advances in the hydration of reactive MgO cement blends incorporating different magnesium carbonates. Constr. Build. Mat. **2021**, 294, 123573. doi.org/10.1016/j.conbuildmat.2021.123573
12. Chaunsali P., Vaishnav K. Calcium-sulfoaluminate-belite cements: opportunities and challenge. The Indian Concr. J. **2020**, 94, 18–25.
13. Gastaldi, D., Bertola, F., Irico, S., Paul, G., Canonico, F. Hydration behavior of cements with reduced clinker factor in mixture with sulfoaluminate binder. Cem. Concr. Res. **2021**, 139, 106261. doi.org/10.1016/j.cemconres.2020.106261
14. Boháč, M.; Staněk, T.; Zezulová, A.; Rybová, A.; Kubátová, D.; Novotný, R. Early Hydration of Activated Belite-Rich Cement. Adv. Mat. Res. **2019**, 1151, 23–27. DOI:10.4028/www.scientific.net/AMR.1151.23

15. Bernardo, G.; Marroccoli, M.; Nobili, M.; Telesca, A.; Valenti, G.L. The use of oil well-derived drilling waste and electric arc furnace slag as alternative raw materials in clinker production. Res. Cons. Rec. **2007**, 52 95–102. doi:10.1016/j.resconrec.2007.02.004.
16. Adolfsson, D.; Menad, N.; Viggh, E.; Bjorkman, B. Steelmaking slags as raw material for sulphoaluminate belite cement. Adv.Cem. Res. **2007**, 19, 147–156, doi:10.1680/adcr.2007.19.4.147.
17. Juenger, M.C.G.; Snellings, R.; Bernal, S.A. Supplementary cementitious materials: New sources, characterization, and performance insights. Cem. Concr. Res. **2019**, 122, 257–273, doi:10.1016/j.cemconres.2019.05.008.
18. Snellings, R.; Suraneni, P.; Skibsted, J. Future and emerging supplementary cementitious materials. Cem. Concr. Res. **2023**, 173, 107199. doi.org/10.1016/j.cemconres.2023.107199.
19. Telesca, A.; Marroccoli, M.; Tomasulo, M.; Valenti, G.L.; Dieter, H.; Montagnaro, F. Low-CO_2 Cements from Fluidized Bed Process Wastes and Other Industrial By-Products. Comb. Sci. Tech. 2016, 188, 492–503, doi:10.1080/00102202.2016.1138736.
20. Telesca, A.; Marroccoli, M.; Pace, M.L.; Tomasulo, M.; Valenti, G.L.; Monteiro, P.J.M. A hydration study of various calcium sulfoaluminate cements. Cem. Concr. Comp. 2014, 53, 224–232.
21. M.K. Mohan, A.V.; Rahul, G.; De Schutter, K.; Van Tittelboom, K. Early age hydration, rheology and pumping characteristics of CSA cement-based 3D printable concrete. Constr. Build. Mat. **2021**, 275, 122136. doi.org/10.1016/ j.conbuildmat.2020.122136.
22. Sirtoli, D.; Wyrzykowski, M.; Riva, P.; Tortelli, S.; Marchi, M.; Lura, P.; Shrinkage and creep of high-performance concrete based on calcium sulfoaluminate cement. Cem. Concr. Comp. **2019**, 98, 61–73. doi.org/10.1016/j. cemconcomp.2019.02.006.
23. Pimraksa, K.; Chindaprasirt, P. 14 - sulfoaluminate cement-based concrete, in: F. Pacheco-Torgal, R.E. Melchers, X. Shi, N.D. Belie, K.V. Tittelboom, A. S´aez (Eds.), Eco-Efficient Repair and Rehabilitation of Concrete Infrastructures, Woodhead Publishing **2018**, 355–385. doi.org/10.1016/B978-0-08- 102181-1.00014-9.
24. Bertola, F.; Gastaldi, D.; Irico, S.; Paul, G.; Canonico, F. Influence of the amount of calcium sulfate on physical/mineralogical properties and carbonation resistance of CSA-based cements. Cem. Concr. Res. **2022**, 151, 106634. doi.org/ 10.1016/j.cemconres.2021.106634.
25. Yang, Z.; Ye, H.; Yuan, Q.; Li, B.; Li, Y.; Zhou, D. Factors influencing the hydration, dimensional stability, and strength development of the OPC-CSA-Anhydrite ternary system. Mat. **2021**, doi.org/10.3390/ma14227001.
26. Tan, B.; Okoronkwo, M.U.; Kumar, A.; Ma, H. Durability of calcium sulfoaluminate cement concrete. J. Zhejiang Univ. - Sci. 21 **2020**, 118–128. doi.org/ 10.1631/jzus.A1900588.
27. Chen, I.A.; Hargis, C.W.; Juenger, M.C.G. Understanding expansion in calcium sulfoaluminate-belite cements. Cem. Concr. Res. **2012**, 42, 51–60. doi:10.1016/j.cemconres.2011.07.010.
28. Wang, L.; Zhan, S.; Tang, X.; Xu, Q.; Qian, K. Pore Solution Chemistry of Calcium Sulfoaluminate Cement and Its Effects on Steel Passivation. Appl. Sci. **2019**, 9, 1092. doi:10.3390/app9061092.
29. Mobili, A.; Belli, A.; Giosué, C.; Telesca, A.; Marroccoli, M.; Tittarelli, F. Calcium sulfoaluminate, geopolimeric, and cementitious mortars for structural applications. Environments **2017**, 4, 64. doi:10.3390/environments4030064.
30. Kiventerä, J.; Piekkari, K.; Isteri, V.; Ohenoja, K.; Tanskanen, P.; Illikainen, M. Solidification/stabilization of gold mine tailings using calcium sulfoaluminate-belite cement. J. Clean. Prod. **2019**, 239, 118008. doi: 10.1016/j.jclepro.2019.118008
31. Tao, Y.; Rahul, A.V.; Mohan, M.K.; De Schutter, G; Van Tittelboom, K. Recent progress and technical challenges in using calcium sulfoaluminate (CSA) cement. Cem. Concr. Comp. **2023**, 137, 104908. doi.org/10.1016/j.cemconcomp.2022.104908.
32. Coppola, L.; Coffetti, D.; Crotti, E. An holistic approach to a sustainable future in concrete construction. IOP Conf. Ser. Mater. Sci. Eng. **2018**, 442, 012024. doi:10.1088/1757-899X/442/1/012024.
33. Ren, C.; Wang, W.; Mao, Y.; Yuan, X.; Song, Z.; Sun, J.; Zhao, X. Comparative life cycle assessment of sulfoaluminate clinker production derived from industrial solid wastes and conventional raw materials, J. Clean. Prod. **2017**, 116, 1314–1324, doi.org/10.1016/j.jclepro.2017.05.184.
34. Marroccoli, M.; Montagnaro, F.; Telesca, A.; Valenti, G.L. Environmental implications of the manufacture of calcium sulfoaluminate-based cements. In Proceedings of the 2nd International Conference on Sustainable Construction Materials and Technologies, Ancona, Italy, 28–30 June **2010**; Zachar, J., Claisse, P., Naik, T.R., Ganjiam, E., Eds.; UWM Center for By-Products Utilization:Milwaukee, WI, USA, 2010.
35. El-Alfi, E.A.; Gado, R.A. Preparation of calcium sulfoaluminate-belite cement from marble sludge waste. Constr. Build. Mat. **2016**, 113, 764–772. doi. org/10.1016/j.conbuildmat.2016.03.103.
36. Isteri, V.; Ohenoja, K.; Hanein, T.; Kinoshita, H.; Tanskanen, P.; Illikainen, M.; Fabritius, T. Production and properties of ferrite-rich CSAB cement from metallurgical industry residues, Sci. Tot. Env. **2020**, 712, 136208. doi.org/10.1016/j.scitotenv.2019.136208.

37. Chen, I.A.; Juenger, M.C.G. Incorporation of coal combustion residuals into calcium sulfoaluminate-belite cement clinkers. Cem. Concr. Comp. **2012**, 34, 893–902. doi.org/10.1016/j.cemconcomp.2012.04.006.
38. Isteri, V.; Ohenoja, K.; Hanein, T.; Kinoshita, H.; Kletti, H.; R¨oßler, C.; Tanskanen, P.; Illikainen, M.; Fabritius, T. Ferritic calcium sulfoaluminate belite cement from metallurgical industry residues and phosphogypsum: clinker production, scale-up, and microstructural characterisation, Cem: Concr. Res. **2022**, 154, 106715. doi.org/10.1016/j.cemconres.2022.106715.
39. Telesca, A.; Marroccoli, M.; Winnefeld, F. Synthesis and characterization of calcium sulfoaluminate cements produced by different chemical gypsums. Adv. Cem. Res. **2019**, 31, 113–123, doi:10.1680/jadcr.18.00122.
40. Telesca, A.; Matschei, T.; Marroccoli, M. Study of eco-friendly belite-calcium sulfoaluminate cements obtained from special wastes. Appl. Sci. **2020**, 10, 8650. doi:10.3390/app10238650
41. Galluccio, S.; Beirau, T.; Pollmann, H. Maximization of the reuse of industrial residues for the production of eco-friendly CSA-belite clinker. Constr. Build. Mater. **2019**, 208, 250–257. doi.org/10.1016/j.conbuildmat.2019.02.148
42. Shen, Y.; Qian, J.; Chai, J.; Fan, Y. Calcium sulphoaluminate cements made with phosphogypsum: production issues and material properties. Cem. Concr. Res. **2014**, 48, 67–74. dx.doi.org/10.1016/j.cemconcomp.2014.01.009
43. Marroccoli, M.; Pace, M.L.; Telesca, A.; Valenti, G.L. Synthesis of calcium sulfoaluminate cements from Al_2O_3-rich by-products from aluminium manufacture. In Proceedings of the 2nd International Conference on Sustainable Construction Materials and Technologies, Ancona, Italy, 28–30 June 2010; Zachar, J., Claisse, P., Naik, T.R., Ganjiam, E., Eds.; UWM Center for By-Products Utilization: Milwaukee, WI, USA, 2010.
44. Arjunan, P.; Silsbee, M.R.; Roy, D.M. Sulfoaluminate-belite cement from low-calcium fly ash and sulfur-rich and other industrial by-products. Cem. Concr. Res. **1999**, 29, 1305–1311.
45. García-Maté, M.; De la Torre, A.G.; Leon-Reina, L.; Aranda, M.A.G.; Santacruz, I. Hydration studies of calcium sulfoaluminate cements blended with fly ash. Cem. Concr. Res. **2013**, 54, 12–20. dx.doi.org/10.1016/j.cemconres.2013.07.010
46. Hargis, C.W.; Telesca, A.; Monteiro, P.J.M. Calcium sulfoaluminate (Ye'elimite) hydration in the presence of gypsum, calcite, and vaterite. Cem. Concr. Res. **2014**, 65, 15–20. dx.doi.org/10.1016/j.cemconres.2014.07.004
47. Lukas, H.J.; Winnefeld, F.; Tschopp, E.; Müller, C.J.; Lothenbach, B. Influence of fly ash on the hydration of calcium sulfoaluminate cement. Cem. Concr. Res. **2017**, Volume 95, pp 152-163. doi.org/10.1016/j.cemconres.2017.02.030
48. Martin, L.H.J.; Winnefeld, F.; Mu¨ller, C.J.; Lothenbach, B. Contribution of limestone to the hydration of calcium sulfoaluminate cement. Cem. Concr. Comp. **2015**, 62, 204–211. dx.doi.org/10.1016/j.cemconcomp.2015.07.005
49. Pelletier-Chaignat, L.; Winnefeld, F.; Lothenbach, B.; Mu¨ller, C.J. Beneficial use of limestone filler with calcium sulfoaluminate cement. Constr. Build. Mat. **2012**, Volume 26, pp 619-627. doi:10.1016/j.conbuildmat.2011.06.065
50. Bertola, F.; Gastaldi, D.; Canonico, F.; Paul, G. CSA and slag: Towards CSA composite binders. Adv. Cem. Res. **2019**, 31, 147–158. https://doi.org/10.1680/jadcr.18.00105
51. Yoon, H.N.; Seo, J.; Kim, S.; Lee, H.K.; Park, S. Hydration of calcium sulfoaluminate cement blended with blast-furnace slag. Const. Build. Mater. **2021**, 268, 121214. dx.doi.org/10.1016/j.conbuildmat.2020.121214
52. Gao, D.; Zhang, Z.; Meng, Y.; Tang, J.; Yang, L. Effect of Flue Gas Desulfurization Gypsum on the Properties of Calcium Sulfoaluminate Cement Blended with Ground Granulated Blast Furnace Slag. Materials **2021**, 14, 382. dx.doi.org/10.3390/ma14020382
53. Kim, T.; Ki_Young, Y.S.; Kang, C.; Lee, T.-K. Development of Eco-Friendly Cement Using a Calcium Sulfoaluminate Expansive Agent Blended with Slag and Silica Fume. Appl. Sci. **2021**, 11, 394. https://doi.org/10.3390/app11010394
54. Anger, B.; Moulin, I.; Commene, J.P.; Thery, F.; Levacher, D. Fine-grained reservoir sediments: an interesting alternative raw material for Portland cement clinker production. Eur. J. Env. Civ. Eng **2017**, DOI: 10.1080/19648189.2017.1327890.
55. Faure, A.; Smith, A.; Coudray, C.; Anger, B.; Colina, H.; Moulin, I.; Thery, F. Ability of Two Dam Fine-Grained Sediments to be Used in Cement Industry as Raw Material for Clinker Production and as Pozzolanic Additional Constituent of Portland-Composite Cement. Waste Biom. Val. **2017**, 8, 2141–2163. doi10.1007/s12649-017-9870-8
56. Snellings, R.; Cizer, O¨.; Horckmans, L.; Durdziński, P.T.; Dierckx, P.; Nielsen, P.; Van Balen, K.; Vandewalle, L. Properties and pozzolanic reactivity of flash calcined dredging sediments. App. Clay Sci. **2016**, 129, 35–39. dx.doi.org/10.1016/j.clay.2016.04.019
57. Mohammed, S. Processing effect and reactivity assessment of artificial pozzolans obtained from clays and clay wastes: A review. Constr. Build. Mat. **2017**, 140, 10-19. dx.doi.org/10.1016/j.conbuildmat.2017.02.078
58. Taylor, H.F.W. Cement Chemistry, 2nd ed.; Academic Press: London, UK, **1997**; p. 480, doi:10.1680/cc.25929.